Am J Cancer Res 2022;12(9):4140-4159
www.ajcr.us /ISSN:2156-6976/ajcr0144372

Original Article

Emerging roles of GALNT5 on promoting EGFR activation in cholangiocarcinoma: a mechanistic insight

Marutpong Detarya[1], Worachart Lert-Itthiporn[1], Panupong Mahalapbutr[1], Methus Klaewkla[2], Supannika Sorin[1], Kanlayanee Sawanyawisuth[1], Atit Silsirivanit[1], Wunchana Seubwai[3], Chaisiri Wongkham[1], Norie Araki[4], Sopit Wongkham[1]

[1]Department of Biochemistry, Faculty of Medicine, and Center for Translational Medicine, Khon Kaen University, Khon Kaen 40002, Thailand; [2]Future Health Innovation Technology Co., Ltd., Bangkok 10170, Thailand; [3]Department of Forensic Medicine, Faculty of Medicine, Khon Kaen University, Khon Kaen 40002, Thailand; [4]Department of Tumor Genetics and Biology, Graduate School of Medical Sciences, Faculty of Life Sciences, Kumamoto University, Kumamoto 860-8556, Japan

Received May 25, 2022; Accepted August 23, 2022; Epub September 15, 2022; Published September 30, 2022

Abstract: Cholangiocarcinoma (CCA) is a lethal cancer in that the incidence is now increasing worldwide. N-acetylgalactosaminyltransferase 5 (GALNT5), an enzyme that initiates the first step of mucin type-O glycosylation, has been reported to promote aggressiveness of CCA cells via the epithelial to the mesenchymal transition (EMT) process, and Akt/Erk activation. In this study, the clinical and biological relevance of GALNT5 and the molecular mechanisms by which GALNT5 modulated EGFR in promoting CCA progression were examined. Using publicly available datasets, upregulation of GALNT5 in patient CCA tissues and its correlation with EGFR expression was noted. High levels of GALNT5 were significantly associated with the short survival of patients, suggesting a prognostic marker of GALNT5 for CCA. GALNT5 modulated EGFR expression as shown in CCA cell lines. Upregulation of GALNT5 significantly increased EGFR mRNA and protein in GALNT5 overexpressing cells, whereas suppression of GALNT5 expression gave the opposite results. The molecular dynamics simulations and MM/PB(GB)SA-based free energy calculations showed that O-glycosylation on the EGFR extracellular domain enhanced the structural stability, compactness, and H-bond formation of the EGF/GalNAc-EGFR complex compared with those of EGF/EGFR. This stabilized the growth factor binding site and fostered stronger interactions between EGF and EGFR. Using the EGF-induced EGFR activation model, GALNT5 was shown to mediate EGFR stability via a decreased rate of EGFR degradation and enhanced EGFR activity by increasing the binding affinity of EGF/EGFR that consequently increasing the activation of EGFR and its downstream effectors Akt and Erk. In summary, GALNT5 was upregulated in CCA tissues and associated with a worse prognosis. The study identified for the first time the impacts of GALNT5 on EGFR activity by increasing: 1) EGFR expression via a transcriptional-dependent mechanism, 2) EGFR stability by reducing EGFR degradation, and 3) EGFR activation through an increased binding affinity of EGF/EGFR which all together fostered the activation of EGFR. These results expanded the understanding of the molecular mechanism of how GALNT5 impacted CCA progression and suggested GALNT5 as a new target for therapeutic intervention against metastatic CCA.

Keywords: O-GalNAcylation, O-glycosylation, glycosyltransferase, EGFR synthesis, EGFR stability, EGFR activation, biliary tract cancer, GALNT5

Introduction

Mucin-type O-glycosylation is a post-translational modification found mostly on membranes and in secretory proteins. The process is initiated by one of the 20 polypeptide N-acetylgalactosaminyltransferase family members (GALNT1-GALNT20) which adds the innermost N-acetylgalactosamine (GalNAc) to serine or threonine residues of the polypeptides. GALNTs are, therefore, the limiting step of O-glycosylation [1, 2]. Although all GALNTs have similar catalytic action, the distinct family member is differentially expressed in the specific tissues and cells, indicating a certain function of the family member in the tissues and cells [1].

Cholangiocarcinoma (CCA), a primary hepatic malignancy of the bile duct epithelia, is a rare tumor worldwide, but is highly prevalent in East

and Southeast Asia, especially in Northeastern Thailand. Chronic biliary tract inflammation due to the infection of liver fluke, *Opisthorchis viverrini*, is a known risk factor for CCA in this area. In other parts of the world, choledocholithiasis, cholelithiasis, and primary chronic sclerosing cholangitis that leads to biliary tract inflammation have been reported to be the risks. The different etiology contributes to the distinct genetic aberrations, clinical presentations and therapeutic approaches between fluke and non-fluke associated CCA [3]. CCA is usually diagnosed when the tumor has progressed to the advanced stages, at which time curative treatment, usually only surgical, can be offered to a limited number of patients [4]. Hence, the understanding of molecular mechanisms inherent the development and progression of CCA are necessary for developing new effective targeted therapy to improve the treatment and patient survival of CCA.

Several growth factors and growth factor receptors are involved in the development of the capabilities for sustaining proliferative signaling and promoting invasion and metastasis of cancer. Among these, epidermal growth factor receptor (EGFR) is commonly overexpressed and associated with progression and poor prognosis in many cancer types, including CCA [5-11]. Activation of EGFR by its ligand, epidermal growth factor (EGF), consequently activated downstream signaling cascades, and promoted CCA growth and metastasis [12, 13]. Several studies have highlighted the significance of O-GalNAcylation on EGFR functions based on the GALNT family members and tumor types. For instance, overexpression of GALNT2 occurs in oral squamous cell carcinoma [14] or up-regulation of GALNT1 in hepatocellular carcinoma (HCC) cells [15] increased O-GalNAcylation on EGFR and enhanced migration and invasion activities of the cancer cells. In contrast, overexpressing GALNT2 and GALNT4 in HCC cells increased O-GalNAcylation on EGFR but suppressed cell growth, migration, and invasion [16, 17].

GALNT5 was identified as the major family member of GALNT associated with aggressive phenotypes of human CCA cell lines [18]. Suppression of GALNT5 significantly reduced proliferation, migration, and invasion, whereas overexpression of GALNT5 exhibited the opposite phenotypes. The mechanism was shown to involve the epithelial-mesenchymal transition process with the increase of Akt and Erk activations. As Akt and Erk signaling are downstream effectors of EGFR, and GALNT5 expression has been shown to be involved with the aggressiveness of CCA. Thus, it was then hypothesized that GALNT5 possibly facilitates the aggressive phenotypes of CCA cells via promoting EGFR activation.

In the present study, the impacts of GALNT5 on EGFR activation were highlighted. The expression and clinical significance of GALNT5 in patients with CCA were analyzed using the publicly available datasets. The molecular dynamics (MD) simulation and free energy calculations were applied to study the effects of O-GalNAcylation on the stability and binding affinity of EGF to EGFR. To gain deeper insight, the influence and biological mechanisms of GALNT5 on EGFR activation were analyzed using the EGF induced EGFR activation model in the GALNT5 knock-down and GALNT5 overexpressing CCA cells.

Materials and methods

CCA cell lines

Cell lines, namely KKU-055, KKU-100, KKU-213A and KKU-213B were established from primary CCA tissues of Thai patients with liver fluke infections [19, 20]. All cell lines were obtained from the Japanese Collection of Research Bioresources (JCBR) Cell Bank, Osaka, Japan. KKU-055 and KKU-100 originated from the poorly differentiated adenocarcinoma CCA, whereas KKU-213A and KKU-213B exhibited poorly differentiated and well differentiated squamous cell carcinoma. Cells were cultured in Ham's F-12 Nutrient Mixture (Gibco; Paisley, Scotland, UK) containing 10% fetal bovine serum (FBS) (Gibco; Paisley, Scotland, UK) and a 1% antibiotic-antimycotic (Gibco), in a humidified incubator at 37°C with 5% CO_2. The Human Research Ethics Committee of Khon Kaen University approved the study protocol (HE641574).

Transcriptomic data sources

The GEO datasets were retrieved using GEO2R [21]. The differential expression of GALNT5 and

EGFR of 91 CCA and normal tissues were compared using the GSE76297 dataset from the Gene Expression Omnibus (GEO) database (https://www.ncbi.nlm.nih.gov/geo/), based on GPL17586 [HTA-2_0] Affymetrix Human Transcriptome Array 2.0 [transcript (gene) version] [22]. The GSE89749 dataset of CCA cases with clinical features and the survival time provided (n = 48) were used for clinical correlation and survival analyses [23]. The expression levels of GALNT5 and EGFR from various tumor *vs.* normal tissues were retrieved from The Cancer Genome Atlas (TCGA, http://gepia.cancer-pku.cn) databases via the GEPIA (Gene Expression Profiling Interactive Analysis) web-based tool [24].

Over-expression and suppression of GALNT5 expression in CCA cells

GALNT5 over-expressing KKU-055 cells and GALNT5 suppressing KKU-213B cells were established as previously described [18]. Briefly, KKU-055 cells were transfected with the pcDNA3.1-GALNT5 and control expression vector. Stable transfected cells with a high expression of GALNT5 were selected and used in the studies. Suppression of GALNT5 in KKU-213B cells was performed using specific siRNA to GALNT5 (5'-CCUGGUUAAGACUUAUUAA-3'). CCA cells (1×10^5 cells/well) cultured in 6-well plates for 18 h and were transfected with 100 pmole of siGALNT5 or si-scramble (Negative Control siRNA, #1027310; Qiagen, Hilden, Germany) using 2 μg/mL of Lipofectamine 2000 (Invitrogen, Carlsbad, CA, USA) according to the recommendations from the manufacturer. The transfection complex was removed after 6 h and cells were cultured in Ham's F-12 medium supplemented with 10% FBS for 48 h before being subjected to subsequent experiments.

EGF treatment

For EGF-induced EGFR activation, cells (2×10^5 cells/well) were cultured in a 6-well plate for 48 h and starved in a serum-free medium overnight. Cells were stimulated with the specified concentration of EGF (PeproTech, Rocky Hill, NJ, USA), in a serum-free medium for 10 min. Cells were then washed with cold phosphate buffer saline (PBS), harvested with a lysis buffer and subsequently subjected to Western blot analysis. For the EGF-induced EGFR degradation model, cells were treated with 100 ng/mL EGF and 20 μg/mL cycloheximide (Sigma-Aldrich, St. Louis, MO, USA) for 0, 0.5, 1, and 2 h. Cells cultured in the serum-free medium without EGF were used as controls.

SDS-PAGE and Western blot analysis

Cell lysis, sodium dodecyl sulphate-polyacrylamide gel electrophoresis (SDS-PAGE) and Western blotting were performed as previously described [18]. Protein (20 μg/well) was subjected to a 10% SDS-PAGE and transferred to polyvinylidene fluoride (PVDF) membranes (Immobilon-P; Millipore, Bedford, MA, USA) by wet electro-transfer using Bolt & Mahoney buffer. Immunodetection of the particular protein was performed using specific monoclonal antibodies as follows: anti-GALNT5 (#HPA008963, 1:500) form Sigma-Aldrich, anti-pEGFR (pY1068, #2234, 1:500), anti-EGFR (#D38B1, 1:1000), anti-pAkt (pS473, #9271, 1:1000), anti-Akt (#9272, 1:1000), anti-pErk1/2 (T202/Y204, #9101, 1:1000), and anti-Erk1/2 (#9102, 1:1000), anti-Claudin-1 (#13255, 1:1000), anti-Slug (#9585, 1:1000) and anti-Vimentin (#5741, 1:1000) from Cell Signaling Technology (Danvers, MA, USA) and anti-GAPDH (#MAB374, 1:5000) from EMD Millipore (Merk KGaA, Darmstadt, Germany). The membranes were probed with each primary antibody at 4°C, overnight and then with horseradish peroxidase (HRP) conjugated secondary antibody, anti-Rabbit (#NA934V, 1:10000; GE Healthcare, Buckinghamshire, UK) or anti-Mouse (#62-6520, 1:10000; Invitrogen) at room temperature for 1 h. Immunoreactivity was detected using the Western HRP substrate (Immobilon Forte; Millipore, Burlington, MA, USA) and analyzed using an ImageQuant LAS 4000 miniimage analyzer (GE Healthcare). ImageQuant TL analysis software (GE Healthcare) was used for semi-quantitative analysis of the images.

RNA extraction and real-time RT-PCR

Total RNA from cell lines was extracted in Trizol® reagent (Invitrogen) and reverse-transcribed using a High-Capacity cDNA Reverse Transcription Kit (Applied biosystems, Carlsbad, CA, USA), according to the manufacturer's

instructions. The PCR reaction was performed as previously described [18, 25], using 50 ng of cDNA, 2.5 μM of forward and reverse primers and LightCycle 480® SYBR green I master mix (Roche Diagnostic, Mannheim, Germany). Primers used were as described previously [18, 25]. The mRNA expression levels of GALNT5 and EGFR were relatively quantified by normalizing with β-actin using LightCycle 480® Relative Quantification software (Roche Diagnostics). Data are mean and S.D. from three independent experiments with duplicated assays each.

EGFR immunocytofluorescent staining

CCA cell lines (2×10^5 cells/well) were cultured in 24-well plates for 24 h and then starved in a serum-free media, overnight. Cells were fixed with 4% ice-cold paraformaldehyde for 15 min at room temperature. The nonspecific glycoconjugate binding was blocked using 5% (v/v) FBS in PBS for 30 min. Then, cells were incubated with anti-EGFR (A-10, 1:500) (Santa Cruz Biotechnology, CA, USA) at 4°C overnight. After washing with PBS, cells were treated with ALEXA® 488 (Invitrogen; CA) and 1 μg/mL of Hoechst 33342 (Molecular Probes; Oregon) at room temperature for 1 h. The fluorescent imaging was determined using a fluorescence microscope (ECLIPSE Ni-U; Nikon, Tokyo, Japan) with Nikon NIS Bioinformatics analysis.

Computational analysis

To predict the O-GalNAcylated sites on EGFR, the amino acid sequences of the extracellular domain of EGFR were first retrieved (NCBI, https://www.ncbi.nlm.nih.gov/protein/NP_005-219.2) and separated into four domains [26]. Crystal structure of human EGFR extracellular domain in complex with EGF (PDB ID: 1IVO [27]) was obtained from the Protein Data Bank. The protonation state of all ionizable amino acid residues was determined at pH 7.4 using H++ server [28]. The GalNAc O-glycosylation sites of EGFR were predicted using the NetOGlyc 4.0 Server [29]. Note that only serine and threonine residues located on the EGFR surface were selected to be O-GalNAcylated by superimposition with the GalNAc-Ser structure (PDB ID: 2D7R) [30] and yielded O-GalNAcylated EGFR (EGFR-GalNAc, **Figure 4A**). Subsequently, the EGFR/EGF and the EGFR-GalNAc/EGF complexes were solvated in an isomeric truncated octahedral TIP3P water box [31] with a spacing distance of 13 Å using a LEaP module in AMBER20. The systems were then neutralized by adding sodium ions. Minimization was performed to remove unfavorable interactions using 2500 steps of steepest descent followed by 2500 steps of conjugated gradient methods.

The MD simulation was performed in the periodic boundary condition with a time step of 2 fs [32] using PMEMD modules implemented in AMBER20. The SHAKE algorithm [33] was used to constrain all bonds involving hydrogen atoms. Temperatures were controlled using the Langevin dynamics technique [34] with a collision frequency of 1 ps^{-1}, in which each system was gradually heated from 10 K to 310 K for 200 ps with a harmonic restraint of 10 kcal/mol·$Å^2$ to the protein backbones. After that, the systems were simulated in NVT ensemble at 310 K for 300 ps followed by an NPT ensembly at 310 K and 1 atm until reaching 50 ns. The CPPTRAJ module of AMBER20 was used to calculate the root-mean-square displacement (RMSD), the number of atomic contacts (# contacts), the number of hydrogen bonds (# H-bonds), and the solvent accessible surface area (SASA) along the simulation times. Note that structural criteria for H-bond calculation are (i) distance between the H-bond donor (HD) and H-bond acceptor (HA) ≤ 3.0 Å and (ii) angle of HD-H·HA ≥ 135°. The EGFR residues located within 5 Å of EGF binding were used as the solvent-exposed area for SASA calculation. The MMPBSA.py module [35] of AMBER20 was employed to calculate the bound free energy (ΔG_{bind}) based on molecular mechanics/Poisson-Boltzmann surface area (MM/PBSA) and the molecular mechanics/generalized Born surface area (MM/GBSA) methods [36], without taking into account the entropic contribution, using 100 frames extracted from the last 10 ns trajectories of the production run.

Statistical analysis

All quantitative data are presented as mean ± standard deviation (SD) of three biologically independent experiments. Statistical analysis was performed using SPSS statistics 24.0 software (IBM Corp., Armonk, NY, USA) and GraphPad Prism 7.0 software (GraphPad Software Inc., San Diego, CA, USA). The Kaplan-

Meier survival plot with the log-rank test was used for survival analysis. The clinicopathological features of patients were compared using the chi-square test. The significance of the data was determined using Student's t-test (two-tailed) and *P* values < 0.05 were considered significant.

Results

GALNT5 was overexpressed in CCA tissues and associated with poor survivals of patients

The differential expression of GALNT family members in CCA tissues vs. non-cancerous regions from CCA patients were analyzed using the GSE76297 dataset (n = 91). CCA tissues that differentially expressed GALNT family members were compared with the non-cancerous tissues (**Figure 1A**). Giving those of the non-cancerous tissues a value of 1, expression level GALNT5 and other 3 GALNTs (GALNT3, GALNT7, and GALNT12) were > 1.4 fold increased in CCA tissues. Most of the CCA tissues exhibited higher GALNT5 expression and lower EGFR expression than those of the non-cancerous counter parts (P < 0.0001, **Figure 1B** and **1C**). The clinical impacts of GALNT5 and EGFR expression were analyzed using the GSE89749 dataset, containing 48 CCA cases with demographics and outcome data provided. Based on the median values of GALNT5 and EGFR expression, univariate analyses demonstrated that the expression level of GALNT5 was not associated with the clinico-pathological features of CCA patients tested except for the expression level of EGFR (P = 0.004). On the contrary, a high EGFR expression was significantly related with the aggressive non-papillary type CCA (P = 0.047) and the expression of GALNT5 (P = 0.004, **Table 1**).

The Kaplan-Meier analysis indicated that patients with high GALNT5 expression had significantly shorter overall survival than those with low GALNT5 (*P* = 0.033, **Figure 1D**), with a median survival time of 278 days (95% confidence interval, CI, 117-378 days) *vs.* 557 days (95% CI, 432-681 days). A similar result was observed in the patients with high EGFR expression (*P* = 0.042, **Figure 1E**), with a median survival time of 340 days (95% CI, 211-468 days) *vs.* 505 days (95% CI, 340-669 days) of those with low EGFR expression. To investigate the connection of GALNT5 and EGFR, the expression levels of EGFR in CCA tissues with low *vs.* high expression of GALNT5 were compared. As depicted in **Figure 1F**, CCA tissues with low GALNT5 expression also had low EGFR expression (P = 0.01). The cooperation of GALNT5 and EGFR expression on patient survival was demonstrated in **Figure 1G**. CCA patients who had high GALNT5 and high EGFR exhibited considerably shorter median survival time than those who had low GALNT5 and low EGFR (*P* = 0.016), with a median survival time 340 days (95% CI, 213-466 days) vs. 609 days (95% CI, 447-770 days). Altogether, these results indicated the association of GALNT5 with EGFR expression in CCA tissues and suggested GALNT5 and EGFR as prognosis markers of CCA patients.

GALNT5 was upregulated in certain cancer tissues and correlated with EGFR expression

As the correlation between EGFR and GALNT5 expression was first noted in this study, whether this finding was specific to CCA or generalized in other cancer tissues was next examined. Expression levels of GALNT5 in tumor *vs.* normal tissues from various cancers were compared using a TCGA dataset with GEPIA analysis. Of 31 cancer types analyzed, tumor tissues of 5 cancers; colon adenocarcinoma, kidney renal papillary cell carcinoma, pancreatic adenocarcinoma, rectum adenocarcinoma and stomach adenocarcinoma had higher expression levels of GALNT5 than the normal tissues (**Figure 2A**) and were significantly correlated with EGFR expression (**Figure 2B**). These results emphasized the connection of GALNT5 and EGFR in cancers with high GALNT5 expression.

GALNT5 mediates EGFR expression in CCA cell lines

To examine the impacts of GALNT5 on EGFR, the basal expression levels of GALNT5 and EGFR in 4 CCA cell lines-namely KKU-055, KKU-100, KKU213A and KKU-213B were first determined. **Figure 3A** shows the Western blots of GALNT5 with two different molecular weight bands. These two bands were shown to be GALNT5 resulting from the different degrees of glycosylation (Supplementary Figure 1). The Western blots (**Figure 3A**) and the quantitative

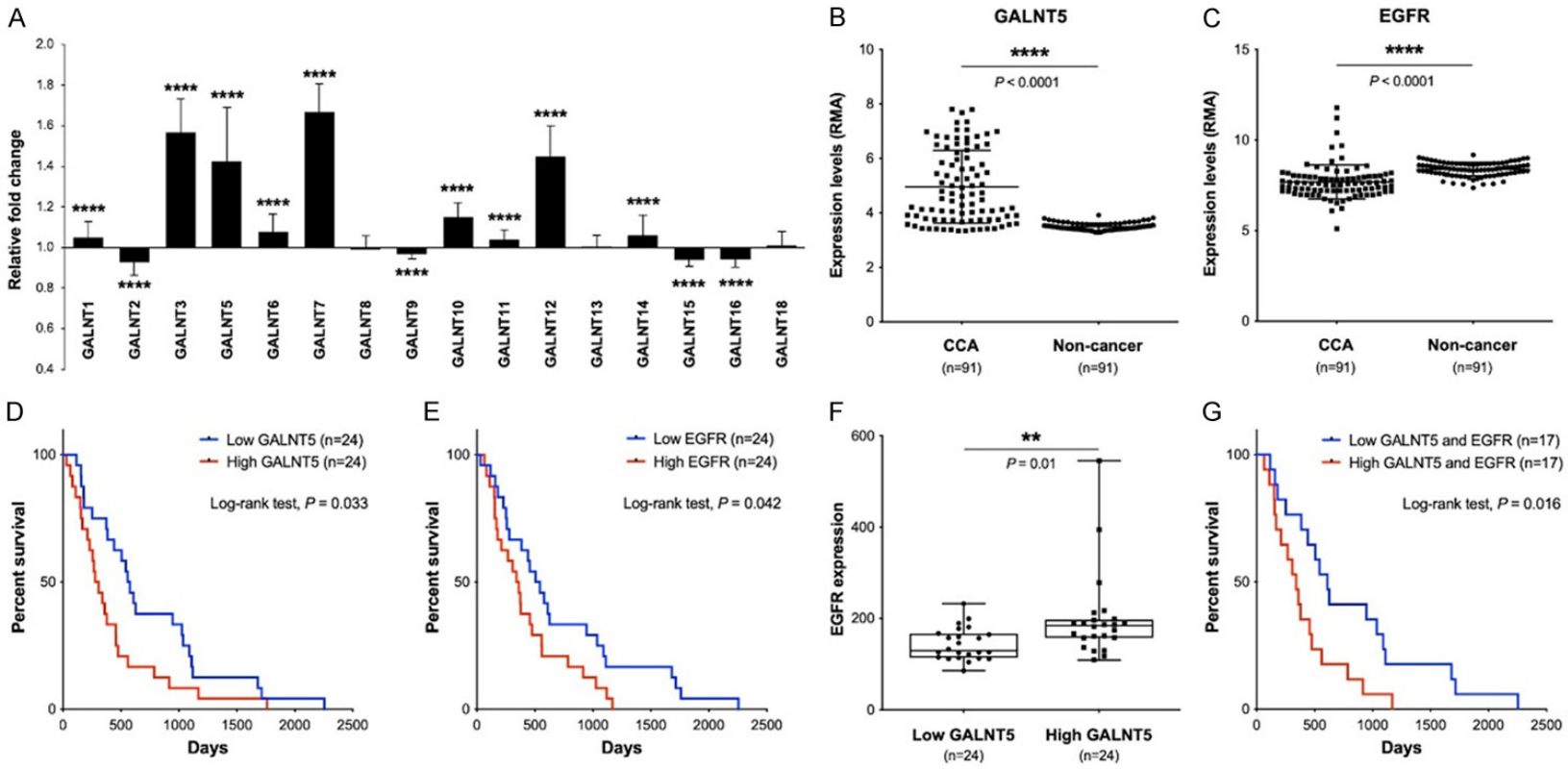

Figure 1. GALNT5 is highly expressed in patient-CCA tissues and associated with poor prognosis. GALNT5 and EGFR expression were retrieved from the GSE76297 dataset (n = 91). (A) Expression of 16 GALNT family members of CCA tissues were compared with the non-cancerous tissues by counting those of normal tissues as 1. (B, C) Expression levels of GALNT5 and EGFR in CCA tissues were compared with those of the non-cancerous regions. (D-G) The data were analyzed using the GSE89749 dataset of CCA patients with clinical findings (n = 48). Patients were divided into 2 groups according to the median values. Kaplan-Meir survival curves with the log-rank test were determined for patients with low and high expression of (D) GALNT5, (E) EGFR and (G) combination of GALNT5 and EGFR. (F) EGFR expression was associated with GALNT5 expression. The data are mean ± S.D. and numbers in the parentheses indicate the number of the samples. RMA = Robust Multi-array Average. $^{**}P = 0.01$, $^{****}P < 0.0001$, Student's *t*-test.

Table 1. Univariate analysis of GALNT5 and EGFR expression in CCA tissues and clinico-pathological findings of patients

Clinical characteristics	No. of patients	GALNT5 expression			EGFR expression		
		Low (n = 24)	High (n = 24)	*P*-value	Low (n = 24)	High (n = 24)	*P*-value
Age (years)							
< 56	24	12	12	0.613	13	11	0.387
≥ 56	24	12	12		11	13	
Gender							
Male	29	15	14	0.500	15	14	0.500
Female	19	10	9		9	10	
Histological type							
Papillary	19	12	7	0.143	13	6	0.047
Non-papillary	28	12	16		11	17	
Tumor stage							
I-III	27	15	12	0.281	13	14	0.500
IVA-B	21	9	12		11	10	
EGFR level							
Low	24	17	7	0.004	-	-	-
High	24	7	17		-	-	
GALNT5 level							
Low	24	-	-	-	17	7	0.004
High	24	-	-		7	17	

analysis (**Figure 3B**) indicated that CCA cell lines differentially expressed GALNT5 and EGFR. Expression of both GALNT5 and EGFR were hardly detected in KKU-055 but were highly expressed in KKU-213B. The low GALNT5 expressing cells (KKU-055 and KKU-100) had significantly lower EGFR expression than the high GALNT5 expressing cells (KKU-213A and KKU-213B) (**Figure 3C**). The results confirmed the link between the expression of GALNT5 and EGFR observed in cancer tissues.

Whether GALNT5 modulated EGFR expression was next validated. EGFR expression in GALNT5 over-expressing KKU-055 cells and GALNT5 suppressed KKU-213B cells were examined in comparison with their control cells. As shown in **Figure 3D** and **3E**, EGFR expressions of the GALNT5 over-expressing cells were significantly higher than those of the control cells. On the contrary, EGFR expression of the GALNT5 suppressing cells was considerably lower than those of the scramble control cells. The results were supported by EGFR-immunocytofluorescent stain depicted in **Figure 3F**. The positive signal of EGFR was gained in the GALNT5 overexpressing cells and was dimmed in the siGALNT5 treated cells. How GALNT5 modulated EGFR expression was next verified. The EGFR-mRNA was determined using the real-time reverse transcriptase-polymerase chain reaction (real-time RT-PCR). The results showed that forced expression of GALNT5 significantly increased EGFR transcripts and *vice versa,* suppressed expression of GALNT5 significantly reduced EGFR-mRNA (**Figure 3G**). Collectively, these results indicated that GALNT5 mediated the transcriptomic and translational levels of EGFR in CCA cells.

Molecular dynamics simulation signified the positive influence of O-GalNAcylation on stability and binding affinity of EGF/EGFR

Even though O-GalNAcylation on EGFR has been demonstrated in several studies [14-17, 37-43], O-GalNAcylated sites on EGFR have never been reported. Using the NetOGly 4.0 Server analyses [29], O-GalNAcylated sites on serine/threonine residues of the EGFR sequence were simulated as shown in **Figure 4A**. There were 17 O-GalNAcylated sites postulated as indicated by yellow squares. Of these, 12 (71.58%) were on the EGF-binding site of the domain 3 (depicted as green fonts). These data suggested that O-GalNAcylation may alter the binding affinity between EGF and EGFR.

As cells differently responded to the O-GalNAcylated EGFR (GalNAc-EGFR) was based

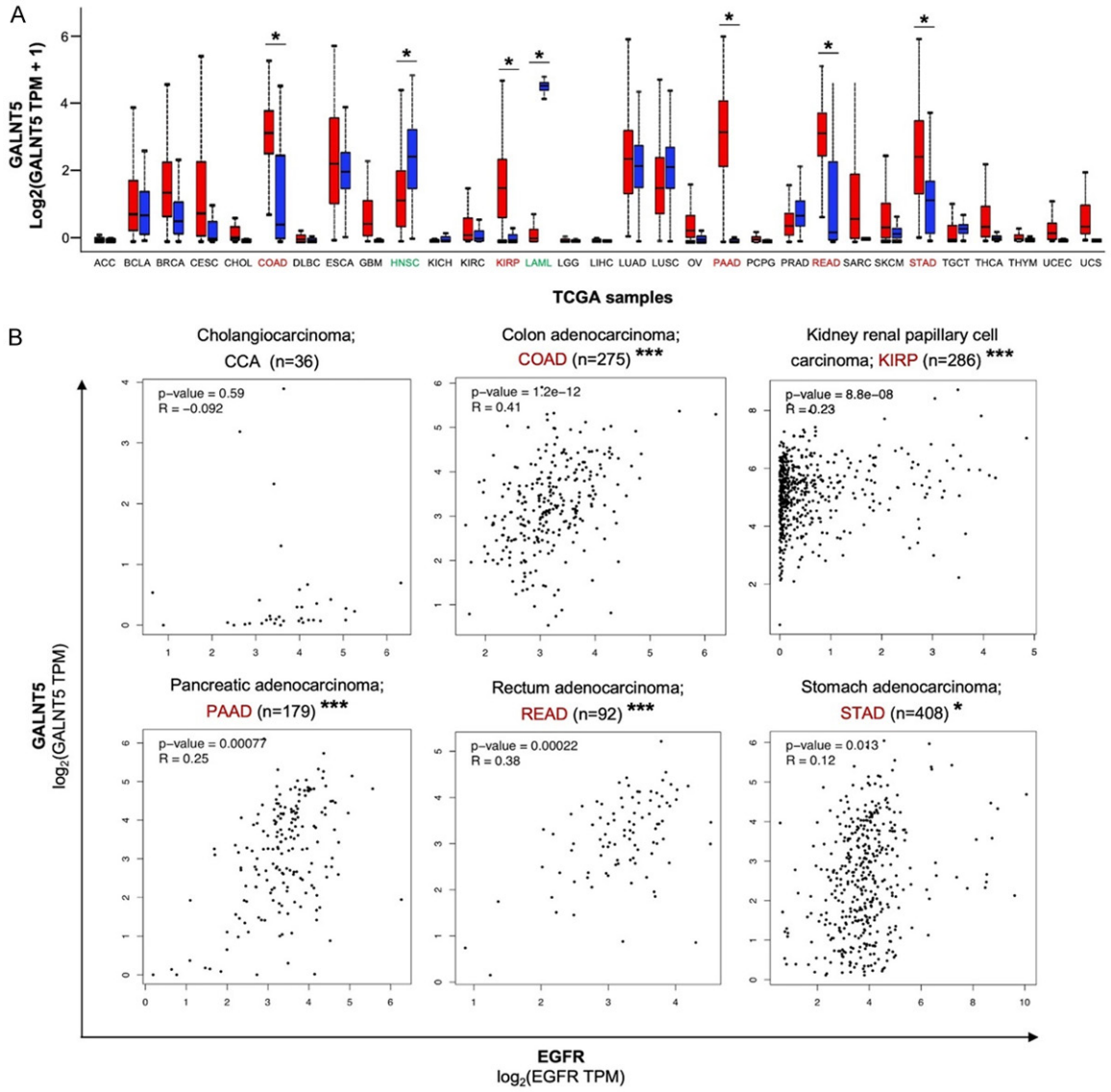

Figure 2. Differential GALNT5 expression in various tumor tissues. The data were analyzed using the TCGA dataset with GEPIA analysis. A. GALNT5 expression in tumor tissues compared with normal counterparts. The differential expression of GALNT5 between tumor (red bar) vs. normal (blue bar) with statistical significance (*, $P < 0.01$) was defined by the font colors; black = not different; red = higher in tumor; green = lower in tumor. B. Correlation analysis of GALNT5 and EGFR expression in cancer tissues. Numbers in the parentheses indicate the number of the samples. TPM = Transcripts Per Million. *$P < 0.05$, ***$P < 0.001$, Student's *t*-test. Abbreviations: ACC, Adrenocortical carcinoma; BLCA, bladder cancer; BRCA, breast cancer; CESC, cervical and endocervical adenocarcinoma; CHOL, cholangiocarcinoma; COAD, colon adenocarcinoma; DLBC, Lymphoid Neoplasm Diffuse Large B-cell Lymphoma; ESCA, esophageal carcinoma; GBM, glioblastoma multiforme; HNSC, head and neck squamous cell carcinoma; KICH, kidney chromophobe; KIRP, kidney renal papillary cell carcinoma; LAML, Acute Myeloid Leukemia; LGG, Brain Lower Grade Glioma; LIHC, liver hepatocellular carcinoma; LUAD, lung adenocarcinoma; LUSC, lung squamous cell carcinoma; OV, Ovarian serous cystadenocarcinoma; PAAD, pancreatic adenocarcinoma; PCPG, pheochromocytoma and paraganglioma; PRAD, prostate adenocarcinoma; READ, rectum adenocarcinoma; SARC, sarcoma; SKCM, skin cutaneous melanoma; SKCM, Skin Cutaneous Melanoma; STAD, stomach adenocarcinoma; THCA, thyroid carcinoma; THYM, thymoma; UCEC, uterine corpus endometrial carcinoma; UCS, Uterine Carcinosarcoma.

on the GALNT family member and cell types; whether GALNT5 contributed to the EGFR stability and activation was first predicted using computational analyses. The *in-silico* models of EGF/EGFR and EGF/GalNAc-EGFR complexes are shown in **Figure 4B**. To investigate the bind-

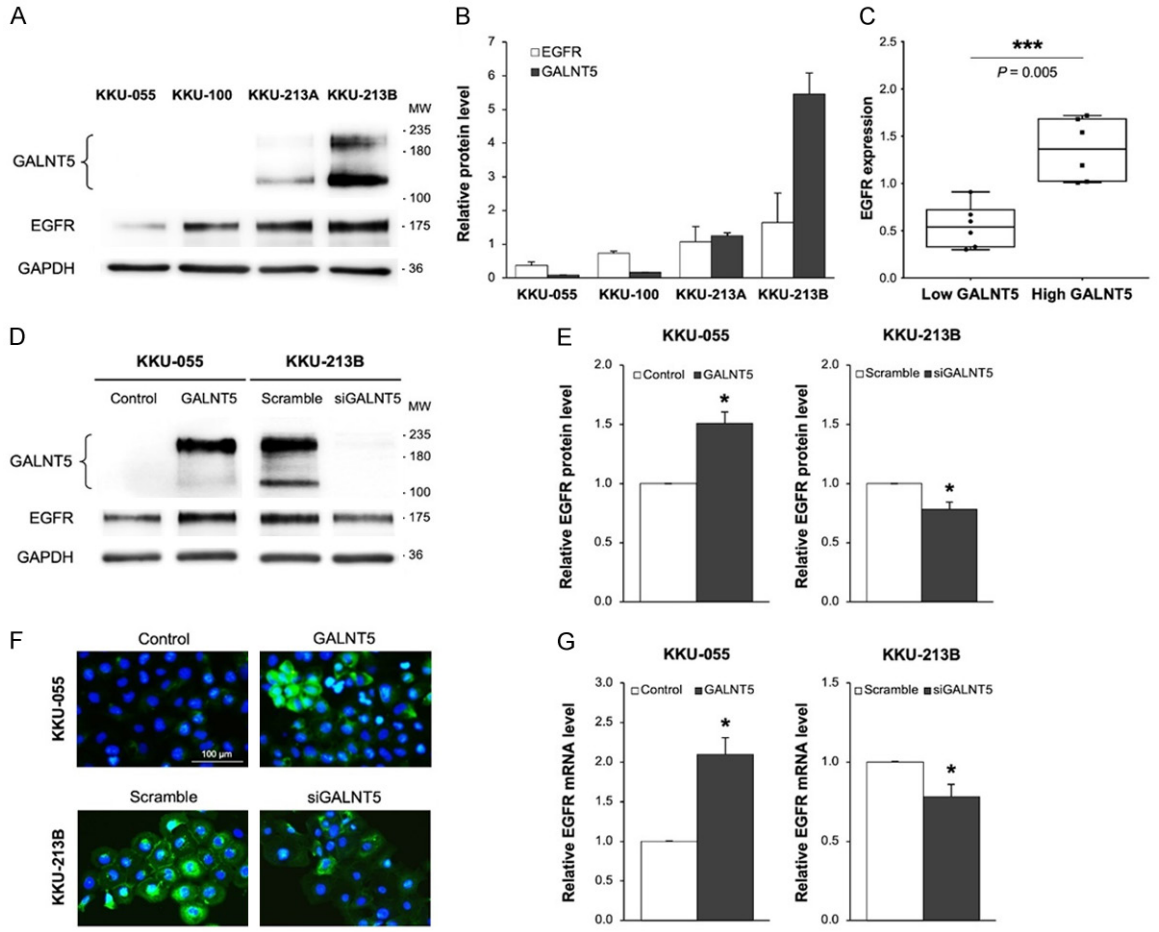

Figure 3. GALNT5 mediates EGFR expression through transcriptional dependence. (A) Western blot of GALNT5 and EGFR expression, and (B) the quantitative analyses were determined in 4 CCA cell lines. (C) GALNT5 expression was divided according to the median values into low and high GALNT5, and the EGFR expression of the two groups were compared. (D, E) Western blot and the quantitative analysis of EGFR and GALNT5, (F) Immunocytofluorescent staining of EGFR and (G) EGFR-mRNA determined using real-time RT-PCR, of the GALNT5 overexpressing KKU-055, and GALNT5 suppressing KKU-213B cells compared with the control cells. The comparative analyses were performed by giving those of the control cells a value of 1. The data are mean ± SD from three independent experiments. * = $P < 0.05$, ***P < 0.001, Student's *t*-test. GALNT5 = GALNT5 over-expressing cells; siGALNT5 = siGALNT5 treated cells; MW = molecular weight in kDa.

ing affinity of EGF against EGFR and GalNAc-EGFR, the MD simulations and free energy calculations based on MM/PBSA and MM/GBSA techniques were performed. Nine serine/threonine residues at the surface of EGFR that could be GalNAcylated *in silico* were used in the simulation (indicated by red dotted line-squares). As shown in **Figure 4C**, the ΔG_{bind} of EGF against GalNAc-EGFR was dramatically lower than that against native EGFR for both calculation methods. This finding was strongly supported by the structural analyses along with the simulation times (**Figure 4D**) demonstrating that the structural stability (RMSD index), compactness, and # H-bonds of the EGF/GalNAc-EGFR complex were higher than those of EGF/EGFR system. Furthermore, the O-GalNAcylation on EGFR extracellular domain exhibited a lower number of water molecules accessible to the binding pocket upon EGF recognition than the unmodified EGFR (SASA index). The O-GalNAcylation modification might enhance the binding ability of EGF ligand. Collectively, these results defined the molecular mechanism by which O-GalNAcylation enhanced the stability and the binding affinity of EGF to GalNAc-EGFR.

GALNT5 promotes stability of EGFR protein

Whether GALNT5 affected the stability of EGFR by decreasing the rate of EGFR degradation was next investigated. Using the EGF-induced

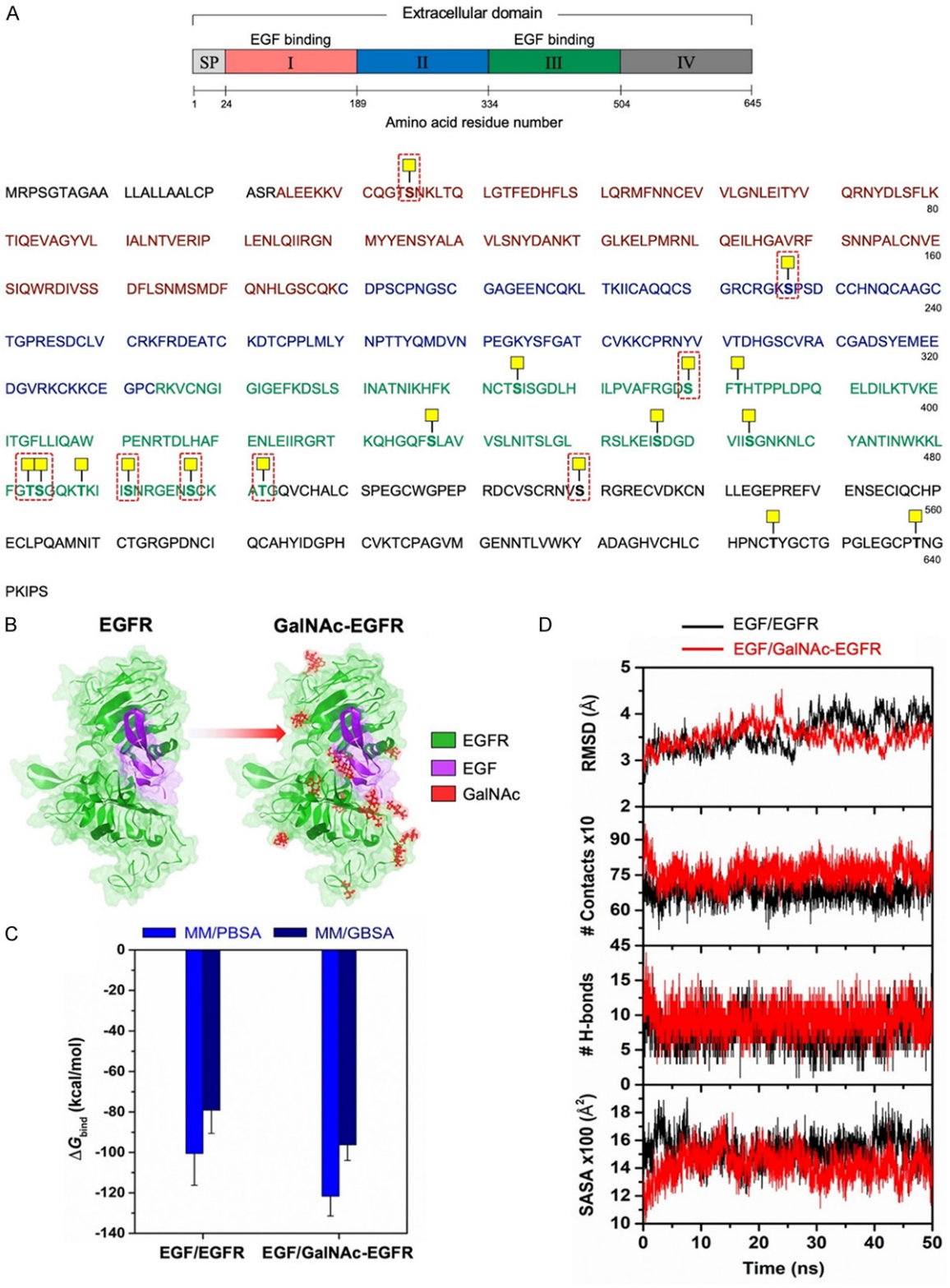

Figure 4. O-GalNAcylation on extracellular domain of EGFR enhances EGF-EGFR binding affinity. A. Schematic diagrams of the extracellular domains and amino acid sequences of EGFR. Yellow squares indicate the predicted O-GalNAcylation sites; red-dash squares indicate the GalNAc residues that were included in MD simulations. B. Structure of EGF binding to EGFR and GalNAc-EGFR. Green = EGFR, purple = EGF, red = GalNAc. C. Binding free energy (ΔG_{bind}) calculations of EGF against EGFR compared with GalNAc-EGFR based on MM/PBSA and MM/GBSA

techniques. D. Structure analyses of EGF binding to EGFR compared with GalNAc-EGFR were calculated by root-mean-square displacement (RMSD), the number of atomic contacts (# contacts), the number of hydrogen bonds (# H-bonds), and the solvent accessible surface area (SASA) along the simulation times. MM = molecular mechanics, PBSA = Poisson-Boltzmann surface area, GBSA = generalized Born surface area.

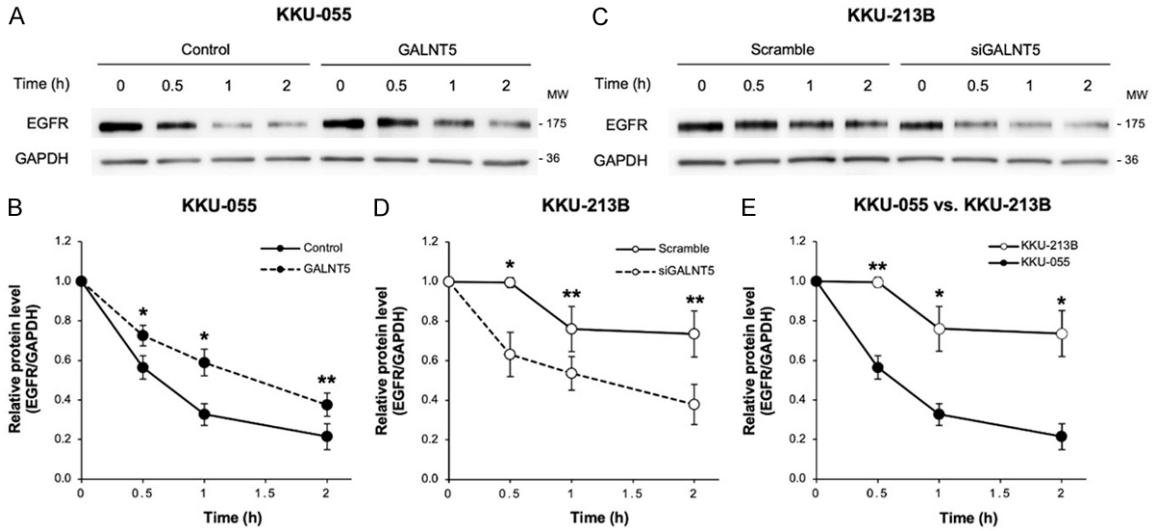

Figure 5. GALNT5 promotes stability of EGFR protein. KKU-055-GALNT5 overexpressing cells, and 48 h-siGALNT5 treated KKU-213B cells together with its controls were starved overnight. Cells were treated with cyclohexamide in the presence of 100 ng/mL of EGF to induce EGFR degradation for 0.5, 1, and 2 h. Western blot and quantitative analysis of EGFR protein were determined in (A, B) GALNT5 over-expressing KKU-055 cells compared with the control cells, (C, D) siGALNT5 KKU-213B cells compared with the scramble control cells. (E) The degradation rates of EGFR protein of KKU-213B and KKU-055 cells were compared. EGFR protein at 0 timepoint was assigned a value of 1. The data are mean ± SD from three independent experiments. * = $P < 0.05$, ** = $P < 0.01$, Student's *t*-test. MW = molecular weight in kDa.

EGFR degradation model, GALNT5 overexpressing KKU-055, the siGALNT5 treated KKU-213B and their control cells were serum starved overnight and treated with EGF 100 ng/mL in the presence of 20 μg/mL cyclohexamide for 0, 0.5, 1, and 2 h. EGFR protein was determined using Western blotting. As shown in **Figure 5A** and **5B**, overexpression of GALNT5 significantly delayed the EGFR degradation rate compared to those of the control cells. EGFR proteins of the control cells were reduced to 56% in 0.5 h and 32% in 1 h, whereas those of the GALNT5 over-expressing cells were maintained at 73% and 59% in 0.5 h and 1 h. On the contrary, suppression of GALNT5 expression significantly accelerated the EGFR degradation rate compared with those of the scramble control cells (**Figure 5C** and **5D**). EGFR proteins of the scramble-control cells were 99% in 0.5 h and 76% in 1 h, whereas those of the siGALNT5 treated cells were 63% in 0.5 h and 54% in 1 h. To affirm this finding, the EGFR degradation rate of KKU-055, the low GALNT5 expressing cells and KKU-213B, the high GALNT5 expressing cells were compared. As shown in **Figure 5E**, KKU-055 exhibited a markedly faster rate of EGFR degradation than KKU-213B. These results indicated the influence of GALNT5 on the EGFR stability.

GALNT5 enhances EGF/EGFR activation

To validate the contribution of GALNT5 on EGFR activation, the short pulse of EGF-induced EGFR activation model was performed. The GALNT5 overexpressing and GALNT5 suppressing cells were serum starved overnight and treated with EGF 100 ng/mL for 10 min. Activations of EGFR and its downstream effectors Akt and Erk signaling were examined using Western blotting. The results shown in **Figure 6A** indicated that EGF treatment could activate EGFR, Akt and Erk signaling of the control and GALNT5 overexpressing cells compared with those without EGF treatment. Giving the activating signals (ratios of pEGFR/EGFR, pAkt/Akt

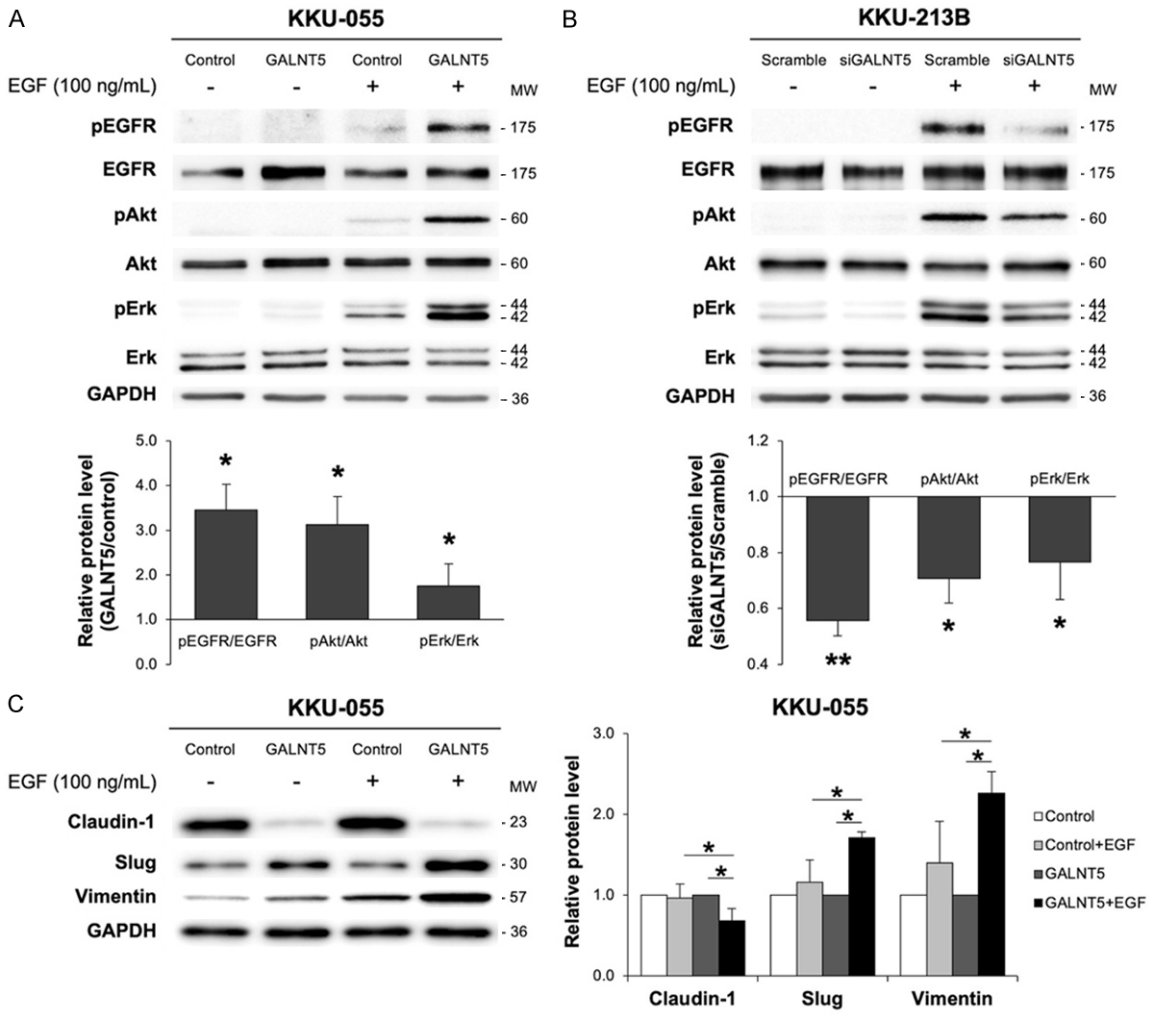

Figure 6. GALNT5 enhances EGF/EGFR activation. KKU-055-GALNT5 overexpressing cells, and 48 h-siGALNT5 treated KKU-213B cells together with its controls were overnight starved. Cells were treated with 100 ng/mL of EGF for 10 min. The total and phosphorylated forms of EGFR and its downstream effectors, Akt and Erk were determined using Western blot. The activating signals were calculated as phosphorylated form/total form by giving those of the EGF activated-control cells a value of 1. (A) KKU-055-GALNT5 overexpressing cells, (B) siGALNT5 treated KKU-213B cells. (C) The effects of EGF treatment on EMT markers in the control and KKU-055-GALNT5 expressing cells, giving the value of the nontreated cells as 1. The data are mean ± SD from three independent experiments. * = $P < 0.05$, ** = $P < 0.01$, Student's *t*-test. GALNT5 = GALNT5 over-expressing cells; siGALNT5 = siGALNT5 treated cells; MW = molecular weight in kDa.

and pErk/Erk) of the EGF treated control cells as 1, all activating signals of the EGF treated GALNT5 overexpressing cells were significantly higher than those of the EGF treated control cells. Conversely, all the activating signals of the EGF treated-siGALNT5 KKU-213B cells were significantly lower than those of the EGF activated-scramble control cells (**Figure 6B**). These results emphasized the impact of GALNT5 on the activation of EGF/EGFR axis.

The molecular mechanism by which GALNT5 and the EGF/EGFR activation acts on the aggressive phenotypes, migration and invasion, was next validated. The expression levels of two epithelial to mesenchymal transition (EMT) markers modulated by GALNT5 expression, claudin-1 and slug [18], were determined in the control *vs.* GALNT5 overexpressing-KKU055 cells, in the presence or absence of EGF. The Western blots and the quantitative analysis shown in **Figure 6C** indicate that expression of slug and vimentin in GALNT5 overexpressing cells was significantly increased while that of claudin-1 was considerably decreased by EGF treatment. A similar trend of

observation was noted in the control pair but without a statistical difference. Moreover, the effects of EGF treatment on these EMT markers in the GALNT5 expressing cells were significantly higher than those of the control cells. These results indicate that the GALNT5 influenced aggressive phenotypes observed in CCA cells [18] were mediated through EGF-EGFR activation.

GALNT5 facilitates the binding affinity of EGF to EGFR

To demonstrate whether GALNT5 promoted EGF/EGFR activation via the increased binding affinity of EGF to EGFR, the EGF-induced EGFR activation model was performed using low to medium doses of EGF treatment. GALNT5 overexpressing KKU-055 cells and GALNT5 knocked-down KKU-213B cells were serum starved overnight and then treated with 5-30 ng/mL EGF for 10 min. The levels of pEGFR, pAkt and pErk were determined using Western blots. As shown in **Figure 7A** and **7B**, EGF treatment could activate EGFR, Akt and Erk phosphorylation as a dose dependent fashion. Notably, at the same dose of EGF treatment, pEGFR/EGFR, pAkt/Akt and pErk/Erk of the GALNT5 overexpressing cells were significantly higher than those observed in the control cells. On the contrary, using the same dose of EGF treatment, activation of EGFR, Akt and Erk were significantly lower in the GALNT5 knocked-down cells compared with those of the scramble control cells (**Figure 7C** and **7D**). These results supported the positive influence of GALNT5 on the binding affinity of EGF to EGFR.

Discussion

O-GalNAcylation, the crucial step of mucin-type O-link glycosylation modification, is catalyzed by a large family of GALNTs. The impacts of abnormal GALNT family members expressed in tumors on the structures and O-glycan profiles involved with carcinogenesis and cancer progression have been repeatedly reported [1, 44, 45]. A previous study by the current authors demonstrated that an increase of O-GalNAcylation was associated with carcinogenesis and progression of CCA in accordance with GALNT5 expression [18]. The mechanism was shown to be related with the activation of Akt and Erk, the downstream effectors of EGFR. In this study, it was further demonstrated that GALNT5 promoted Akt/Erk activation and progression of CCA cells by influencing EGFR synthesis and activity. The impacts of GALNT5 on EGFR expression, stability, EGF/EGFR binding affinity and EGFR activation were revealed in-depth.

GALNT5 is generally expressed in the mucus secreting cells of gastrointestinal tract, e.g., esophagus, stomach, colon, and lung [1]. Although several GALNT family members have been shown to be associated with malignant phenotypes [44, 45], the reports on GALNT5 in cancer are limited. In CCA, GALNT5 was found to be the major member of GALNTs and associated with the pro-metastatic phenotypes involved with migration and invasion of human CCA cell lines [18]. The clinical impact of GALNT5 on the unsatisfactory outcomes of CCA patients is the first evidence in this study. Using GEO microarray datasets (GSE76297, GSE89749), upregulation and a worse prognostic value of GALNT5 for CCA were identified (**Figure 1B** and **1D**). This observation is in accordance with the *in vitro* findings of Detarya, 2020.

The association of high EGFR expression with progression and poor prognosis of CCA and various cancers are frequently reported [5-11]. In the current study, high EGFR expression was significantly related with poor survival of CCA patients (**Figure 1E**). The prognosis was even worse in the patients who exhibited upregulation of both GALNT5 and EGFR (**Figure 1G**). In addition, the association of GALNT5 expression with EGFR in CCA tissues was identified for the first time in this study (**Figure 1F**; **Table 1**). Apart from CCA, the online analysis of GEPIA showed a positive correlation between GALNT5 and EGFR expression in several cancer types that possessed high GALNT5 (**Figure 2B**). These data suggest the collaborative function between GALNT5 and EGFR and indicate that this finding is not unique to CCA but is common in other cancers.

The Western blot of GALNT5 presented in **Figure 3** showed 2 bands of GALNT5 with different degrees of glycosylation. The images of both Western blot bands disappeared in the siGALNT5 treated KKU-213B cells and appeared in the GALNT5 overexpressing KKU-055 cells (**Figure 3D**). The mobility of the high molecular weight-GALNT5 band was shipped down in the neuraminidase-treated cells and

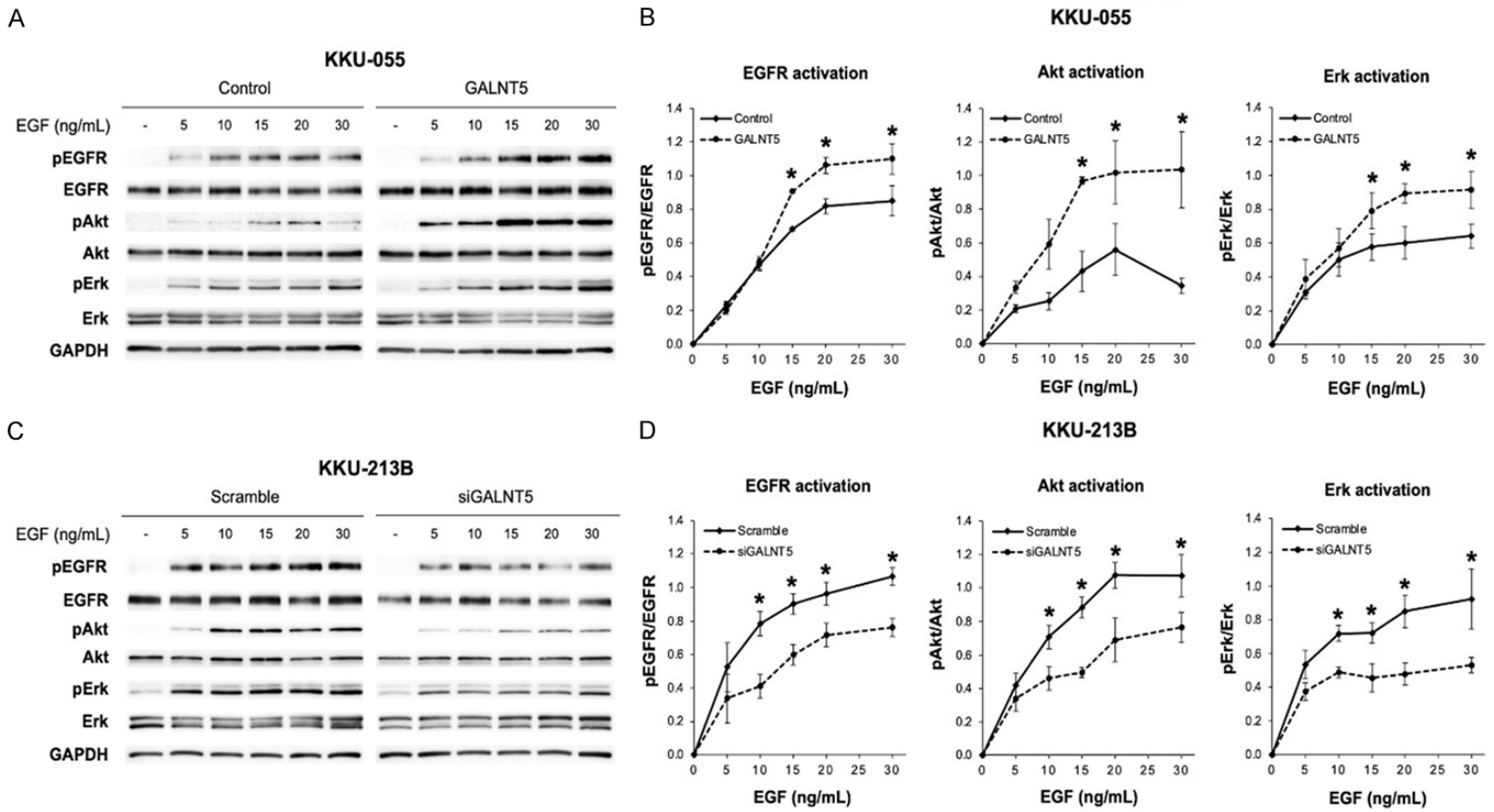

Figure 7. GALNT5 facilitates the binding affinity and activation of EGF/EGFR. KKU-055-GALNT5 overexpressing cells, and 48 h-siGALNT5 treated KKU-213B cells together with its controls were starved overnight. Cells were treated with 5, 10, 15, 20, 30 ng/mL of EGF for 10 min. The total and phosphorylated forms of EGFR and its downstream effectors, Akt and Erk were determined using Western blot. The activating signals were calculated as phosphorylated form/total form by giving those of the non-EGF activated cells as references. (A, B) KKU-055-GALNT5 overexpressing cells, (C, D) siGALNT5 treated KKU-213B cells. The data are mean ± SD from three independent experiments. * = $P < 0.05$, Student's *t*-test.

moved further down to the same position as the lower GALNT5 band after PNGase-F treatment (Supplementary Figure 1). The data indicated GALNT5, a highly glycosylated protein with sialylation and N-liked glycosylation. The finding agreed with the data described in the Uniport indicating that GALNT5 was modified by N-linked glycosylation (https://www.uniprot.org/uniprotkb/Q7Z7M9/entry). In addition, O-linked glycosylation of GALNT5 has been reported recently [46].

Given the finding that expression of GALNT5 was significantly correlated with that of EGFR, a series of experiments was performed to elucidate the cellular and molecular mechanisms underlying this observation. Differential expression of GALNT5 was observed in CCA cell lines with different histological type origins. Remarkably, the expression levels of EGFR corresponded with those of GALNT5 (**Figure 3A-C**). The strong link between GALNT5 and the association with EGFR was further tightened by the fact that the expression level of EGFR was monitored by modulating the expression of GALNT5 (**Figure 3D-F**). Further experiments using quantitative real-time RT-PCR showed that GALNT5 regulated the expression level of EGFR via increased EGFR-mRNA (**Figure 3G**). These findings indicated for the first time of the positive regulation of GALNT5 on EGFR expression in CCA cells via a transcriptomic-dependent mechanism. The exact pathways behind the upregulation of EGFR-mRNA by GALNT5, however, are yet to be fully elucidated.

Several previous studies demonstrated the association of GALNTs on malignant phenotypes via EGFR signaling without interfering with EGFR expression. Knockdown of GALNT1 suppressed malignant phenotypes of HCC and EGFR signaling without affecting expression levels of EGFR mRNA and protein [15]. Similar observations were shown in ovarian cancer cells in that silencing or overexpressing GALNT6 significantly affected progression of cancer cells in accordance with reduction of EGFR activity but not EGFR expression [42]. Also, reduced expression of GALNT4 was significantly associated with adverse survival of patients and promoted malignant phenotypes of HCC without affecting EGFR expression [17]. To the best of the authors knowledge, the positive regulation of a GALNT member on EGFR expression observed in CCA was in accord with the reports of GALNT7 in cervical [47] and papillary thyroid cancers [48]. High expression of GALNT7 was associated with aggressive malignant phenotypes and the increase of EGFR protein. The GEPIA analysis when using a TCGA-THCA dataset, a positive correlation of GALNT7 expression and EGFR in the papillary thyroid tumor was noted.

Each GALNT family member affects cancer differently in the cell context-specific and cell type-specific manner. Aberrant expression of a specific GALNT can be either a tumor promoter or tumor suppressor based on the tumor types and the influence on EGFR. Modification of O-GalNAcylation on EGFR can either positively or negatively affect EGFR function. In HCC, increase of GALNT1 and GALNT10 enhanced the activation and stability of EGFR [15, 39], while those of GALNT2 and GALNT4 showed the opposite effects [16, 17]. On the other hand, a specified GALNT member presented in different cancer types exhibited different outcomes. Overexpression of GALNT2 acted as a tumor suppressor in HCC but acted as a tumor promotor in oral squamous cell carcinoma [14] and glioma cells [37]. These discordant observations highlight the fact that each GALNT family member might have different specific preferences for GalNAc-modification sites on EGFR and interfere with the function of EGFR differently. Although, the exact GalNAcylated sites on EGFR have not yet been elucidated, at least 17 potential GalNAcylation sites were suggested for the first time (**Figure 4A**). The *in-silico* findings of GalNAcylation on EGFR stability were confirmed using an EGF-induced EGFR degradation model (**Figure 5**). The GALNT5 overexpressing cells exhibited lower EGFR-degradation than the control cells, and the opposite results were obtained for the GALNT5 suppressing cells. Also, KKU-213B with high GALNT5 possessed higher EGFR stability than the KKU-055 cells with low GALNT5. The contribution of different GALNT members to the stability of several proteins including EGFR has been repeatedly reported [40, 49, 50]. For instance, the knockdown of GALNT14 in ovarian cancer cells decreased the stability of EGFR [40]. The expression of GALNT6 was shown to contribute to mammary carcinogenesis and stabilize MUC1 protein in breast cancer cells

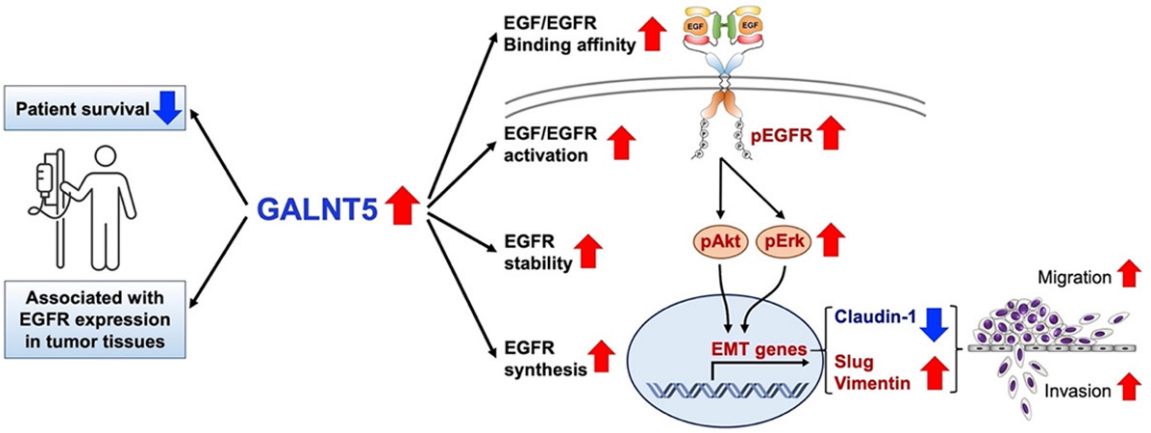

Figure 8. The schematic diagram depicts the impacts of GALNT5 on cholangiocarcinoma progression via EGFR activation. GALNT5 is overexpressed in CCA tissues, associated with EGFR expression and short survival of patients. GALNT5 promotes EGF/EGFR action by increasing the binding affinity and activation of EGF to EGFR, EGFR stability, and synthesis. Activation of Akt and Erk induces EMT process which finally promotes cell migration and invasion.

[49]. In addition, GalNAcylation by GALNT6 could stabilize the GRP78 protein in mammary cancer cells [50]. Even though, not much is known about the mechanism of how GalNAcylation enhanced the stability of proteins, the molecular dynamics simulation presented in **Figure 4B-D** provided for the first time the molecular mechanism by which O-GalNAcylation positively influenced the stability and binding affinity of EGF/EGFR, leading to a strong EGFR activation in GALNT5 expressing cells. To this end, the potential mechanisms that GALNT5 enhanced EGFR expression are the increasing synthesis and decrease of the degradation of EGFR.

The ΔG_{bind}, compactness, # H-bonds, and the number of water molecules accessible to the binding pocket of GalNAc-EGFR upon EGF recognition, were observed from the MD simulation and free energy analyses directed to the conclusion that O-GalNAcylation modification might enhance and stabilize the binding of EGF ligand to GalNAc-EGFR. The possible influence of O-GalNAcylation on stronger binding and activation of EGF/GalNAc-EGFR than EGF/EGFR was proven in the current study by the fact that the activation signal of EGFR, and its downstream effectors Akt and Erk were much stronger in the GALNT5 overexpressing cells, and significantly weaker in the GALNT5 suppressing cells (**Figure 6**). Moreover, upon similar doses of EGF stimulation, a higher EGFR activation was observed in CCA cells with higher GALNT5 expression (**Figure 7**).

GALNT5 modulating progressive phenotypes of CCA cells has been shown previously to be via EMT. Claudin-1, an epithelial marker, was suppressed, whereas those of the mesenchymal markers, slug and vimentin, were upregulated in the GALNT5 overexpressing cells and vice versa in the siGALNT5 treated cells [18]. In this study, the connection of GALNT5 and the EMT activation was further demonstrated to be partly through EGF/EGFR activation. GALNT5 enhanced EGFR function and consequently motivated EMT process, through suppression of claudin-1 and induction of slug and vimentin (**Figure 6C**). Slug is a transcription factor that plays a central role in the EMT and is the downstream mediator of EGFR [51], whereas claudin-1 is a direct downstream target gene of slug [52]. Slug positively regulates vimentin and negatively mediates claudin-1 [53, 54]. Decreased claudin-1 expression under EGFR activation in human bronchial epithelial cells, both in vitro and in vivo [55] supported currently reported findings. Moreover, a stronger activation of EMT in GALNT5 overexpressing cells than the control cells implied the contribution of GALNT5 on EGFR activation.

Collectively, this study shows for the first time of the impacts of GALNT5 expression on the binding affinity, stability, and biological function of EGFR which subsequently activates the EMT process (**Figure 8**). This study, however, has some limitations. All the datasets of CCA patients and human CCA cell lines were from Thai patients that were assumed to be related

with the liver fluke infection. The public datasets of CCA patients, GSE76297, contained only intra-hepatic CCA whereas those from GSE89749 with clinical information were from both intra- and extra-hepatic CCA. Although O-GalNAcylated EGFR in CCA cell lines was not illustrated in this study, the potential GalNAcylation sites and the molecular mechanism postulated by molecular dynamics simulation indicated the positive influence of O-GalNAcylation on EGF/EGFR activation. Nevertheless, the impact of GALNT5 on the biology and function of EGFR as suggested from the *in-silico* findings were confirmed by several experimental model systems used in this study (**Figures 5**-**7**). Also, it cannot rule out that glycoproteins other than EGFR might influence the malignant phenotype associated with GALNT5. At present, the specific substrate of GALNT5 is not clarified and is worthwhile to study further.

In conclusion, this study establishes several novel findings. GALNT5 in patient-CCA tissues was upregulated, associated with poor survival of patients, and positively correlated with EGFR expression. GALNT5 enhances progressiveness of CCA cells, at least in part, through the positive regulation of EGFR transcription, stability, and EGF/EGFR binding affinity. Further animal studies are warranted to prove the impacts of GALNT5 on EGFR function and CCA progression. GALNT5 together with EGFR may be potential targets for controlling CCA progression, especially in patients with high GALNT5 expression.

Acknowledgements

The authors would like to thank Dr. Thanapon Charoenwongpaiboon, Department of Chemistry, Faculty of Science, Silpakorn University, for computing resources, and Prof. James A Will for editing this manuscript via the Faculty of Medicine Publication Clinic, KKU (PCO-957).

Disclosure of conflict of interest

None.

Address correspondence to: Sopit Wongkham, Department of Biochemistry, Faculty of Medicine, Khon Kaen University, Khon Kaen 40002, Thailand. Tel: +66-4334-8386; Fax: +66-4334-8386; E-mail: sopit@kku.ac.th

References

[1] Bennett EP, Mandel U, Clausen H, Gerken TA, Fritz TA and Tabak LA. Control of mucin-type O-glycosylation: a classification of the polypeptide GalNAc-transferase gene family. Glycobiology 2012; 22: 736-756.

[2] Van den Steen P, Rudd PM, Dwek RA and Opdenakker G. Concepts and principles of O-linked glycosylation. Crit Rev Biochem Mol Biol 1998; 33: 151-208.

[3] Brindley PJ, Bachini M, Ilyas SI, Khan SA, Loukas A, Sirica AE, Teh BT, Wongkham S and Gores GJ. Cholangiocarcinoma. Nat Rev Dis Primers 2021; 7: 65.

[4] Luvira V, Nilprapha K, Bhudhisawasdi V, Pugkhem A, Chamadol N and Kamsa-ard S. Cholangiocarcinoma patient outcome in Northeastern Thailand: single-center prospective study. Asian Pac J Cancer Prev 2016; 17: 401-406.

[5] Boonsri B, Yacqub-Usman K, Thintharua P, Myint KZ, Sae-Lao T, Collier P, Suriyonplengsaeng C, Larbcharoensub N, Balasubramanian B, Venkatraman S, Egbuniwe IU, Gomez D, Mukherjee A, Kumkate S, Janvilisri T, Zaitoun AM, Kuakpaetoon T, Tohtong R, Grabowska AM, Bates DO and Wongprasert K. Effect of combining EGFR tyrosine kinase inhibitors and cytotoxic agents on cholangiocarcinoma cells. Cancer Res Treat 2021; 53: 457-470.

[6] Gomes RV, Rodrigues MA, Rodrigues J, Vidigal PT, Damasceno KA, Lima HA, Gomes DA, Machado CJ and Resende V. Expression of epidermal growth factor receptor (EGFR) in cholangiocarcinomas: predictive factors and survival. Rev Col Bras Cir 2018; 45: e1826.

[7] Xu L, Hausmann M, Dietmaier W, Kellermeier S, Pesch T, Stieber-Gunckel M, Lippert E, Klebl F and Rogler G. Expression of growth factor receptors and targeting of EGFR in cholangiocarcinoma cell lines. BMC Cancer 2010; 10: 302.

[8] Yang X, Wang W, Wang C, Wang L, Yang M, Qi M, Su H, Sun X, Liu Z, Zhang J, Qin X and Han B. Characterization of EGFR family gene aberrations in cholangiocarcinoma. Oncol Rep 2014; 32: 700-708.

[9] Hoffmann AC, Goekkurt E, Danenberg PV, Lehmann S, Ehninger G, Aust DE and Stoehlmacher-Williams J. EGFR, FLT1 and heparanase as markers identifying patients at risk of short survival in cholangiocarcinoma. PLoS One 2013; 8: e64186.

[10] Padthaisong S, Thanee M, Techasen A, Namwat N, Yongvanit P, Liwatthakun A, Hankla K, Sangkhamanon S and Loilome W. Nimotuzumab inhibits cholangiocarcinoma cell metastasis via suppression of the epithelial-mesenchymal transition process. Anticancer Res 2017; 37: 3591-3597.

[11] Yoshikawa D, Ojima H, Iwasaki M, Hiraoka N, Kosuge T, Kasai S, Hirohashi S and Shibata T. Clinicopathological and prognostic significance of EGFR, VEGF, and HER2 expression in cholangiocarcinoma. Br J Cancer 2008; 98: 418-425.

[12] Claperon A, Mergey M, Nguyen Ho-Bouldoires TH, Vignjevic D, Wendum D, Chretien Y, Merabtene F, Frazao A, Paradis V, Housset C, Guedj N and Fouassier L. EGF/EGFR axis contributes to the progression of cholangiocarcinoma through the induction of an epithelial-mesenchymal transition. J Hepatol 2014; 61: 325-332.

[13] Yoon JH, Gwak GY, Lee HS, Bronk SF, Werneburg NW and Gores GJ. Enhanced epidermal growth factor receptor activation in human cholangiocarcinoma cells. J Hepatol 2004; 41: 808-814.

[14] Lin MC, Huang MJ, Liu CH, Yang TL and Huang MC. GALNT2 enhances migration and invasion of oral squamous cell carcinoma by regulating EGFR glycosylation and activity. Oral Oncol 2014; 50: 478-484.

[15] Huang MJ, Hu RH, Chou CH, Hsu CL, Liu YW, Huang J, Hung JS, Lai IR, Juan HF, Yu SL, Wu YM and Huang MC. Knockdown of GALNT1 suppresses malignant phenotype of hepatocellular carcinoma by suppressing EGFR signaling. Oncotarget 2015; 6: 5650-5665.

[16] Wu YM, Liu CH, Hu RH, Huang MJ, Lee JJ, Chen CH, Huang J, Lai HS, Lee PH, Hsu WM, Huang HC and Huang MC. Mucin glycosylating enzyme GALNT2 regulates the malignant character of hepatocellular carcinoma by modifying the EGF receptor. Cancer Res 2011; 71: 7270-7279.

[17] Liu Y, Liu H, Yang L, Wu Q, Liu W, Fu Q, Zhang W, Zhang H, Xu J and Gu J. Loss of N-acetylgalactosaminyltransferase-4 orchestrates oncogenic microRNA-9 in hepatocellular carcinoma. J Biol Chem 2017; 292: 3186-3200.

[18] Detarya M, Sawanyawisuth K, Aphivatanasiri C, Chuangchaiya S, Saranaruk P, Sukprasert L, Silsirivanit A, Araki N, Wongkham S and Wongkham C. The O-GalNAcylating enzyme GALNT5 mediates carcinogenesis and progression of cholangiocarcinoma via activation of AKT/ERK signaling. Glycobiology 2020; 30: 312-324.

[19] Sripa B, Leungwattanawanit S, Nitta T, Wongkham C, Bhudhisawasdi V, Puapairoj A, Sripa C and Miwa M. Establishment and characterization of an opisthorchiasis-associated cholangiocarcinoma cell line (KKU-100). World J Gastroenterol 2005; 11: 3392-3397.

[20] Sripa B, Seubwai W, Vaeteewoottacharn K, Sawanyawisuth K, Silsirivanit A, Kaewkong W, Muisuk K, Dana P, Phoomak C, Lert-Itthiporn W, Luvira V, Pairojkul C, Teh BT, Wongkham S, Okada S and Chamgramol Y. Functional and genetic characterization of three cell lines derived from a single tumor of an Opisthorchis viverrini-associated cholangiocarcinoma patient. Hum Cell 2020; 33: 695-708.

[21] Barrett T, Wilhite SE, Ledoux P, Evangelista C, Kim IF, Tomashevsky M, Marshall KA, Phillippy KH, Sherman PM, Holko M, Yefanov A, Lee H, Zhang N, Robertson CL, Serova N, Davis S and Soboleva A. NCBI GEO: archive for functional genomics data sets-update. Nucleic Acids Res 2012; 41: D991-D995.

[22] Chaisaingmongkol J, Budhu A, Dang H, Rabibhadana S, Pupacdi B, Kwon SM, Forgues M, Pomyen Y, Bhudhisawasdi V, Lertprasertsuke N, Chotirosniramit A, Pairojkul C, Auewarakul CU, Sricharunrat T, Phornphutkul K, Sangrajrang S, Cam M, He P, Hewitt SM, Ylaya K, Wu X, Andersen JB, Thorgeirsson SS, Waterfall JJ, Zhu YJ, Walling J, Stevenson HS, Edelman D, Meltzer PS, Loffredo CA, Hama N, Shibata T, Wiltrout RH, Harris CC, Mahidol C, Ruchirawat M and Wang XW; TIGER-LC Consortium. Common molecular subtypes among Asian hepatocellular carcinoma and cholangiocarcinoma. Cancer Cell 2017; 32: 57-70, e53.

[23] Jusakul A, Cutcutache I, Yong CH, Lim JQ, Huang MN, Padmanabhan N, Nellore V, Kongpetch S, Ng AWT, Ng LM, Choo SP, Myint SS, Thanan R, Nagarajan S, Lim WK, Ng CCY, Boot A, Liu M, Ong CK, Rajasegaran V, Lie S, Lim AST, Lim TH, Tan J, Loh JL, McPherson JR, Khuntikeo N, Bhudhisawasdi V, Yongvanit P, Wongkham S, Totoki Y, Nakamura H, Arai Y, Yamasaki S, Chow PK, Chung AYF, Ooi L, Lim KH, Dima S, Duda DG, Popescu I, Broet P, Hsieh SY, Yu MC, Scarpa A, Lai J, Luo DX, Carvalho AL, Vettore AL, Rhee H, Park YN, Alexandrov LB, Gordan R, Rozen SG, Shibata T, Pairojkul C, Teh BT and Tan P. Whole-genome and epigenomic landscapes of etiologically distinct subtypes of cholangiocarcinoma. Cancer Discov 2017; 7: 1116-1135.

[24] Tang Z, Li C, Kang B, Gao G, Li C and Zhang Z. GEPIA: a web server for cancer and normal gene expression profiling and interactive analyses. Nucleic Acids Res 2017; 45: W98-W102.

[25] Detarya M, Thaenkaew S, Seubwai W, Indramanee S, Phoomak C, Saengboonmee C, Wongkham S and Wongkham C. High glucose upregulates FOXM1 expression via EGFR/STAT3 dependent activation to promote progression of cholangiocarcinoma. Life Sci 2021; 271: 119114.

[26] Purba ER, Saita EI and Maruyama IN. Activation of the EGF receptor by ligand binding and oncogenic mutations: the "Rotation Model". Cells 2017; 6: 13.

[27] Ogiso H, Ishitani R, Nureki O, Fukai S, Yamanaka M, Kim JH, Saito K, Sakamoto A, Inoue M, Shirouzu M and Yokoyama S. Crystal structure of the complex of human epidermal growth factor and receptor extracellular domains. Cell 2002; 110: 775-787.

[28] Anandakrishnan R, Aguilar B and Onufriev AV. H++ 3.0: automating pK prediction and the preparation of biomolecular structures for atomistic molecular modeling and simulations. Nucleic Acids Res 2012; 40: W537-541.

[29] Steentoft C, Vakhrushev SY, Joshi HJ, Kong Y, Vester-Christensen MB, Schjoldager KT, Lavrsen K, Dabelsteen S, Pedersen NB, Marcos-Silva L, Gupta R, Bennett EP, Mandel U, Brunak S, Wandall HH, Levery SB and Clausen H. Precision mapping of the human O-GalNAc glycoproteome through SimpleCell technology. EMBO J 2013; 32: 1478-1488.

[30] Kubota T, Shiba T, Sugioka S, Furukawa S, Sawaki H, Kato R, Wakatsuki S and Narimatsu H. Structural basis of carbohydrate transfer activity by human UDP-GalNAc: polypeptide alpha-N-acetylgalactosaminyltransferase (pp-GalNAc-T10). J Mol Biol 2006; 359: 708-727.

[31] Jorgensen WL, Chandrasekhar J, Madura JD, Impey RW and Klein ML. Comparison of simple potential functions for simulating liquid water. J Chem Phys 1983; 79: 926-935.

[32] Mahalapbutr P, Lee VS and Rungrotmongkol T. Binding hotspot and activation mechanism of maltitol and lactitol toward the human sweet taste receptor. J Agric Food Chem 2020; 68: 7974-7983.

[33] York DM, Darden TA and Pedersen LG. The effect of long-range electrostatic interactions in simulations of macromolecular crystals: a comparison of the Ewald and truncated list methods. J Chem Phys 1993; 99: 8345-8348.

[34] Wu X and Brooks BR. Self-guided Langevin dynamics simulation method. Chem Phys Lett 2003; 381: 512-518.

[35] Miller BR 3rd, McGee TD Jr, Swails JM, Homeyer N, Gohlke H and Roitberg AE. MMPBSA.py: an efficient program for end-state free energy calculations. J Chem Theory Comput 2012; 8: 3314-3321.

[36] Genheden S and Ryde U. The MM/PBSA and MM/GBSA methods to estimate ligand-binding affinities. Expert Opin Drug Discov 2015; 10: 449-461.

[37] Sun Z, Xue H, Wei Y, Wang C, Yu R, Wang C, Wang S, Xu J, Qian M, Meng Q and Li G. Mucin O-glycosylating enzyme GALNT2 facilitates the malignant character of glioma by activating the EGFR/PI3K/Akt/mTOR axis. Clin Sci (Lond) 2019; 133: 1167-1184.

[38] Hu WT, Yeh CC, Liu SY, Huang MC and Lai IR. The O-glycosylating enzyme GALNT2 suppresses the malignancy of gastric adenocarcinoma by reducing EGFR activities. Am J Cancer Res 2018; 8: 1739-1751.

[39] Wu Q, Liu HO, Liu YD, Liu WS, Pan D, Zhang WJ, Yang L, Fu Q, Xu JJ and Gu JX. Decreased expression of hepatocyte nuclear factor 4alpha (Hnf4alpha)/microRNA-122 (miR-122) axis in hepatitis B virus-associated hepatocellular carcinoma enhances potential oncogenic GALNT10 protein activity. J Biol Chem 2015; 290: 1170-1185.

[40] Li HW, Liu MB, Jiang X, Song T, Feng SX, Wu JY, Deng PF and Wang XY. GALNT14 regulates ferroptosis and apoptosis of ovarian cancer through the EGFR/mTOR pathway. Future Oncol 2022; 18: 149-161.

[41] Chugh S, Meza J, Sheinin YM, Ponnusamy MP and Batra SK. Loss of N-acetylgalactosaminyltransferase 3 in poorly differentiated pancreatic cancer: augmented aggressiveness and aberrant ErbB family glycosylation. Br J Cancer 2016; 114: 1376-1386.

[42] Lin TC, Chen ST, Huang MC, Huang J, Hsu CL, Juan HF, Lin HH and Chen CH. GALNT6 expression enhances aggressive phenotypes of ovarian cancer cells by regulating EGFR activity. Oncotarget 2017; 8: 42588-42601.

[43] Huang T, Meng F, Huang H, Wang L, Wang L, Liu Y, Liu Y, Wang J, Li W, Zhang J and Liu Y. GALNT8 suppresses breast cancer cell metastasis potential by regulating EGFR O-GalNAcylation. Biochem Biophys Res Commun 2022; 601: 16-23.

[44] Beaman EM and Brooks SA. The extended pp-GalNAc-T family and their functional involvement in the metastatic cascade. Histol Histopathol 2014; 29: 293-304.

[45] Hussain MR, Hoessli DC and Fang M. N-acetylgalactosaminyltransferases in cancer. Oncotarget 2016; 7: 54067-54081.

[46] Bagdonaite I, Pallesen EM, Ye Z, Vakhrushev SY, Marinova IN, Nielsen MI, Kramer SH, Pedersen SF, Joshi HJ, Bennett EP, Dabelsteen S and Wandall HH. O-glycan initiation directs distinct biological pathways and controls epithelial differentiation. EMBO Rep 2020; 21: e48885.

[47] Cao Q, Wang N, Ren L, Tian J, Yang S and Cheng H. miR-125a-5p post-transcriptionally suppresses GALNT7 to inhibit proliferation and invasion in cervical cancer cells via the EGFR/PI3K/AKT pathway. Cancer Cell Int 2020; 20: 117.

[48] Wang Y, Wang C, Fu Z, Zhang S and Chen J. miR-30b-5p inhibits proliferation, invasion, and migration of papillary thyroid cancer by targeting GALNT7 via the EGFR/PI3K/AKT pathway. Cancer Cell Int 2021; 21: 618.

[49] Park JH, Nishidate T, Kijima K, Ohashi T, Takegawa K, Fujikane T, Hirata K, Nakamura Y and Katagiri T. Critical roles of mucin 1 glycosylation by transactivated polypeptide N-acetylgalactosaminyltransferase 6 in mammary carcinogenesis. Cancer Res 2010; 70: 2759-2769.
[50] Lin J, Chung S, Ueda K, Matsuda K, Nakamura Y and Park JH. GALNT6 stabilizes GRP78 protein by O-glycosylation and enhances its activity to suppress apoptosis under stress condition. Neoplasia 2017; 19: 43-53.
[51] Kusewitt DF, Choi C, Newkirk KM, Leroy P, Li Y, Chavez MG and Hudson LG. Slug/Snai2 is a downstream mediator of epidermal growth factor receptor-stimulated reepithelialization. J Invest Dermatol 2009; 129: 491-495.
[52] Martinez-Estrada OM, Culleres A, Soriano FX, Peinado H, Bolos V, Martinez FO, Reina M, Cano A, Fabre M and Vilaro S. The transcription factors Slug and Snail act as repressors of Claudin-1 expression in epithelial cells. Biochem J 2006; 394: 449-457.
[53] Vuoriluoto K, Haugen H, Kiviluoto S, Mpindi JP, Nevo J, Gjerdrum C, Tiron C, Lorens JB and Ivaska J. Vimentin regulates EMT induction by Slug and oncogenic H-Ras and migration by governing Axl expression in breast cancer. Oncogene 2011; 30: 1436-1448.
[54] Virtakoivu R, Mai A, Mattila E, De Franceschi N, Imanishi SY, Corthals G, Kaukonen R, Saari M, Cheng F, Torvaldson E, Kosma VM, Mannermaa A, Muharram G, Gilles C, Eriksson J, Soini Y, Lorens JB and Ivaska J. Vimentin-ERK signaling uncouples slug gene regulatory function. Cancer Res 2015; 75: 2349-2362.
[55] Jia Z, Bao K, Wei P, Yu X, Zhang Y, Wang X, Wang X, Yao L, Li L, Wu P, Yuan W, Wang S, Zheng J, Hua Y and Hong M. EGFR activation-induced decreases in claudin1 promote MUC5AC expression and exacerbate asthma in mice. Mucosal Immunol 2021; 14: 125-134.

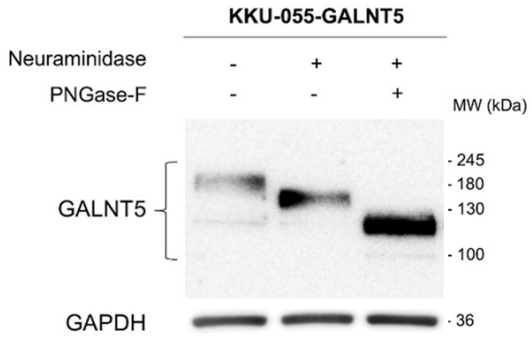

Supplementary Figure 1. Cell lysate of 200 µg was diluted in a 10x GlycoBuffer (0.5 M Sodium Phosphate, pH 7.5) and treated with a final concentration of 50 mU Neuraminidase (Roche) at 37 °C, 1 h. For double enzymatic treatment, after Neuraminidase treatment, N-Glycosidase F (Boehringer, Mannheim) was added to a final concentration of 500 mU at 37 °C, 1 h. The reaction was stopped and subjected to Western blot analysis.